Virology 620 (2026) 110903

Contents lists available at ScienceDirect

Virology

journal homepage: www.elsevier.com/locate/virology

Brief Communication

Leaf bleaching is associated with extensive transcriptional reprogramming in avocado trees with sunblotch disease

M. Joubert [a,b], N. van den Berg [a,b], J. Theron [a], V. Swart [a,b,*]

[a] Department of Biochemistry, Genetics and Microbiology, Faculty of Natural and Agricultural Sciences, University of Pretoria, Pretoria, Gauteng, South Africa
[b] Forestry and Agricultural Biotechnology Institute, University of Pretoria, Pretoria, Gauteng, South Africa

ARTICLE INFO

Keywords:
Avocado sunblotch viroid
ASBVd
Avocado sunblotch disease
Persea americana
RNA-Seq
Transcriptome analysis
Viroid infection

ABSTRACT

Avocado sunblotch viroid (ASBVd), the type member of the family *Avsunviroidae*, causes avocado sunblotch disease; marked by the appearance of distinct chlorotic symptoms on fruit, stems and/or leaves of infected trees. Despite the economic impact of the disease, limited information is available regarding the molecular interactions underlying ASBVd infection of avocado. However, studies of other host-viroid pathosystems have revealed large-scale changes to plant gene expression in response to viroid infection. To elucidate molecular changes associated with sunblotch symptom development, we used next-generation sequencing to investigate the global gene expression differences associated with leaf bleaching symptoms in avocado. A total of 3169 genes were differentially expressed in yellow (chlorotic) tissues of bleached leaves compared to asymptomatic leaves from the same ASBVd-infected trees, with most of these genes being upregulated in chlorotic samples. Grouping of genes by predicted function identified substantial alterations to expression of genes involved in genetic information processing, host immune responses, and photosynthesis. Notably, downregulation of chloroplast-associated genes was linked to the manifestation of leaf bleaching. This is the first study to report on global transcriptome changes associated with a symptomatic avsunviroid infection, and provides new insights into the molecular mechanisms underpinning ASBVd-induced chlorosis.

1. Introduction

Viroids are highly structured, circular single-stranded RNA molecules which represent the smallest known plant pathogens. The 45 viroid species currently recognised are classified into two families, distinguished based on their secondary structures, mode and site of replication in host cells, and conserved genome motifs. Members of the family *Pospiviroidae* (40 species) replicate in host nuclei using an asymmetrical rolling-circle mechanism (Di Serio et al., 2021), whereas members of the family *Avsunviroidae* (5 species) replicate in host chloroplasts using a symmetrical rolling-circle mechanism and display self-cleavage enabled by hammerhead ribozyme activity (Di Serio et al., 2018). These two viroid families are further differentiated by the types of symptoms they trigger in plants, likely linked to their mechanism of pathogenesis (Flores et al., 2020).

The exemplar member of the family *Avsunviroidae*, avocado sunblotch viroid (ASBVd), is the causal agent of avocado sunblotch disease (Allen et al., 1981; Palukaitis et al., 1979). In avocado (*Persea americana* Mill.), the disease manifests through a suite of chlorotic symptoms, including white to red coloured sunken lesions on the fruit, yellow streaking of immature stems, and/or malformed, discoloured leaves (Kuhn et al., 2017). Although the majority of foliage on symptomatic ASBVd-infected trees usually resembles the green leaves of healthy trees, chlorotic leaves may exhibit bleached lesions with sharply defined margins separating yellow and green tissues, or variegated patterns, characterised by mosaic-like chlorosis across the leaf surface (Semancik and Szychowski, 1994). ASBVd infection may also be asymptomatic for extended periods, in which case trees remain free of any chlorosis and act as symptomless carriers of the pathogen (Kuhn et al., 2017).

Investigations into the mechanism of pathogenesis of avsunviroids have shown that RNA silencing is responsible for localised leaf chlorosis characteristic of these infections. Studies of peach infected with peach latent mosaic viroid (PLMVd) and chrysanthemum infected with chrysanthemum chlorotic mottle viroid (CChMVd) proved that viroid RNAs are cleaved by host proteins into viroid-derived small RNAs (vd-sRNAs). These vd-sRNAs subsequently target nuclear-encoded chloroplastic

* Corresponding author. Department of Biochemistry, Genetics and Microbiology, Faculty of Natural and Agricultural Sciences, University of Pretoria, Pretoria, Gauteng, South Africa.
E-mail address: velushka.swart@fabi.up.ac.za (V. Swart).

https://doi.org/10.1016/j.virol.2026.110903
Received 16 February 2026; Received in revised form 2 April 2026; Accepted 7 April 2026
Available online 8 April 2026

transcripts for degradation, leading to chlorotic symptoms (Delgado et al., 2019; Navarro et al., 2012; Serra et al., 2023). Similarly, ASBVd-associated leaf bleaching has been shown to correlate with the presence of numerous ASBVd-derived sRNAs, supporting the role of RNA silencing in triggering leaf chlorosis in avocado sunblotch disease (Joubert et al., 2025; Markarian et al., 2004).

While the precise role of RNA silencing in eliciting the systemic symptoms associated with pospiviroid infection remains unclear (Flores et al., 2020), several studies have investigated host gene expression to gain insight into viroid-induced changes in diseased plants. Using next-generation sequencing (NGS) technologies, global transcriptomic responses have been analysed in plants infected with potato spindle tuber viroid (PSTVd) (Chi et al., 2022; Góra-Sochacka et al., 2019; Hadjieva et al., 2021; Więsyk et al., 2020), hop stunt viroid (HSVd) (Márquez-Molins et al., 2023; Xia et al., 2017; Xu et al., 2020), citrus bark cracking viroid (CBCVd) (Mishra et al., 2018; Štajner et al., 2019), citrus exocortis viroid (CEVd) (Wang et al., 2019), and chrysanthemum stunt viroid (CSVd) (Takino et al., 2019). These studies revealed commonalities in host responses to viroid infection, including differential expression of genes involved in plant defence and stress responses, phytohormone signalling, secondary metabolism, transcription and translation, protein modification and degradation, cell wall structure and photosynthesis (reviewed by Joubert et al. (2022)).

In a previous study, we presented the first NGS-based global transcriptome analysis of an avsunviroid-infected host, examining asymptomatic avocado trees infected with ASBVd. That work revealed that the host pathways affected in ASBVd-infected symptomless-carrier trees largely overlapped with those observed in pospiviroid-host interactions; however, the extent of transcriptome changes was substantially reduced when compared to symptomatic viroid infections (Joubert et al., 2024). To our knowledge, no studies have characterised global gene expression changes associated with a symptomatic avsunviroid infection.

Here we investigate the genome-wide transcriptome changes associated with the development of leaf bleaching symptoms in avocado sunblotch disease. Using RNA-sequencing (RNA-seq), we analysed the expression of avocado genes in yellow tissues of bleached ASBVd-infected leaves compared to green leaf tissues from the same diseased trees. Our results reveal extensive transcriptomic reprogramming in chlorotic tissues, closely resembling the gene expression patterns reported for other symptomatic viroid-host systems. These findings provide new perspectives on the impact of ASBVd infection on the avocado transcriptome, and highlight correlations between the development of leaf bleaching symptoms and host gene expression, thereby advancing our knowledge of viroid-induced pathogenesis in avocado.

2. Materials and methods

Leaf material was collected previously (Joubert et al., 2025) in December 2023 from three avocado trees exhibiting sunblotch symptoms, including bleached and variegated leaves. Trees were located in a single row within one orchard block in Tzaneen, Limpopo province, South Africa. All leaves displaying distinct bleaching symptoms were harvested from each of the three trees, and the yellow (chlorotic) sectors of all available bleached leaves were separated from adjacent green sectors. Leaf material from each sector type was pooled for each tree (representing individual biological replicates) to generate SY samples (yellow sectors of bleached leaves) and SG samples (green sectors of bleached leaves). In addition, five fully green, asymptomatic leaves were collected from representative branches of each tree and pooled to form AS (asymptomatic) samples.

For ASBVd detection, total RNA was extracted from a portion of each of the nine processed samples (SY, SG and AS pooled separately for each of the three trees). For each sample, 400 ng of RNA was used for ASBVd cDNA synthesis, followed by semi-quantitative real-time PCR, as previously described (Joubert et al., 2025).

The remaining ground leaf material was submitted to Macrogen Genome Center (Seoul, Republic of Korea), where total RNA was extracted from all samples. RNA libraries were prepared using the TruSeq Stranded mRNA Library Prep kit (Illumina, San Diego, California, USA). Paired-end sequencing (2 x 150 bp) was performed on the Illumina NovaSeqX platform. Processing of RNA-seq data and differential gene expression (DGE) analysis were performed as previously described (Joubert et al., 2025). DGE was analysed for SY and SG samples relative to AS samples, as well as for SY samples relative to SG samples. Genes were considered differentially expressed in respective datasets if the adjusted *p*-value (*p*adj) was < 0.05 and $\log_2$(Fold Change) ($\log_2$FC) ≥ 1 or ≤ -1.

For functional classification of differentially expressed genes (DEGs), the GOSeq package (Young et al., 2010) in RStudio v2024.04.2.764 (Posit Team, 2024) was used for Gene Ontology (GO) and Kyoto Encyclopedia of Genes and Genomes (KEGG) enrichment analysis. Terms were considered significantly enriched if false discovery rate (FDR) was < 0.05 among up- or downregulated DEGs in each dataset. Further functional categorisation of DEGs was carried out in MapMan v3.6.0RC1 (Schwacke et al., 2019) using functional bins previously assigned to avocado proteins (Backer et al., 2022) through Mercator v3.6 (Lohse et al., 2014). Figures used to map functional pathways in MapMan were created using BioRender (https://biorender.com/shortURL).

3. Results

ASBVd was detected in all symptomatic samples (SY and SG, Fig. 1A), but in only one asymptomatic (AS) sample, originating from Tree 2 (Table S1). Semi-quantitative real-time PCR revealed that ASBVd accumulation was the highest in SY (yellow sector) samples, while SG (green sector) samples from the same leaves consistently had lower viroid titres. Amplification results for AS samples from Tree 1 and 3 were identical to uninfected and non-template controls, while Tree 2_AS had the lowest detectable viroid titre.

RNA-seq produced 40.3 – 43.5 million raw reads per sample. After processing, 40.0 – 43.1 million reads were retained, of which 93% were successfully aligned to the Peame105 avocado genome (Avocado Genome Consortium, personal communication) (Table S2).

Expression analysis of mapped and quantified reads identified a total of 3720 DEGs (*p*adj < 0.05; $|\log_2 FC| \geq 1$), all of which were differentially expressed in yellow (SY) tissues in at least one comparison (Fig. 1B; Table S3). The majority of DEGs (85%) showed altered expression in SY samples relative to AS samples (SY vs AS), while differential expression in green sectors was negligible, with only seven DEGs detected in the SG vs AS comparison. Most DEGs were upregulated in yellow tissues, whether compared to asymptomatic samples (66% of DEGs in SY vs AS) or green sectors of bleached leaves (67% of DEGs in SY vs SG) (Fig. 1C). Comparison of expression data to those obtained in a previous experiment (Joubert et al., 2024) showed that 82 of the DEGs found in bleached tissues were also differentially expressed in asymptomatic trees compared to uninfected counterparts, though with varying trends in their expression (Table S3).

Principal component analysis (PCA) of transformed DGE data from symptomatic trees showed clear separation of samples according to tissue type, with sample origin accounting for 79% of the variance observed (Fig. 1D). Gene expression profiles of yellow (SY) tissues clustered distinctly from those of both green tissues (SG and AS), correlating with the number of DEGs observed in different datasets.

Functional classification of DEGs was carried out to identify cellular pathways and processes which were specifically altered in bleached leaf tissues (Fig. 2, Fig. S1). GO enrichment analysis revealed a greater number of significantly enriched GO terms among upregulated DEGs than among downregulated DEGs in both the SY vs AS (Table S4) and SY vs SG (Table S5) comparisons. The top enriched GO terms (by number of DEGs) for genes upregulated in SY samples were predominantly associated with protein modification and kinase activity, as well as DNA binding and transcription (Fig. 2A, Fig. S1A). In contrast, enriched GO

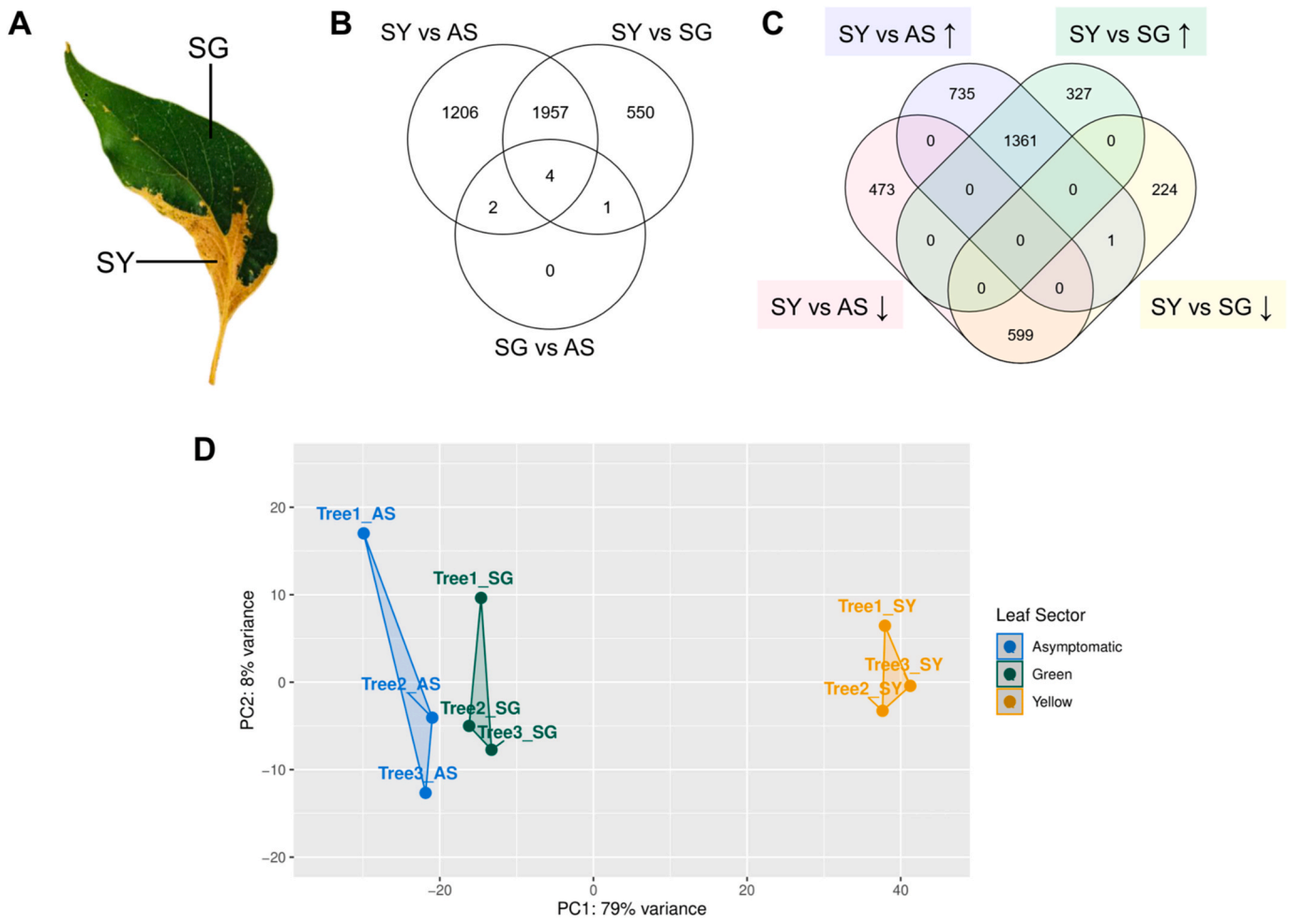

Fig. 1. Comparison of differentially expressed genes (DEGs) observed in different leaf tissue types in avocado trees with sunblotch symptoms. (**A**) Gene expression was analysed separately in yellow (SY) and green (SG) sectors of bleached leaves, and in asymptomatic (AS) leaves (not shown) from three biological replicates. (**B**) Venn diagram comparing the number of DEGs (padj < 0.05; $|\log_2(\text{Fold Change})| \geq 1$) in three analysed datasets: SY relative to AS, SY relative to SG, and SG relative to AS. (**C**) Venn diagram showing the number of up- and downregulated DEGs in SY samples relative to AS and SG samples, respectively. Genes that were significantly upregulated are shown by ↑, while downregulated genes are indicated by ↓. (**D**) Principal component analysis (PCA) showing variation in gene expression in individual samples, plotted using variance-stabilising transformation of DEGs. (For interpretation of the references to colour in this figure legend, the reader is referred to the Web version of this article.)

terms among downregulated DEGs were associated with processes and functions in photosynthesis, or components of host chloroplasts, with disruption of the photosynthetic pathway and machinery being most pronounced in SY samples compared to AS samples (Fig. 2B, Fig. S1B).

Results of KEGG enrichment analysis corroborated the results of GO enrichment, showing that pathways associated with mitogen-activated protein kinase (MAPK) signalling and genetic information processing were over-represented among DEGs upregulated in SY samples relative to both AS and SG samples (Table S6). Other notable KEGG pathways significantly enriched among upregulated DEGs in the SY vs AS comparison included those related to plant-pathogen interactions, secondary metabolism, and transport (Table S6). No KEGG pathways were enriched among downregulated DEGs in our data.

Further functional categorisation was performed using MapMan, allowing a more comprehensive overview of the DEGs with roles in particular plant processes (Fig. 2C, Fig. S1C). MapMan visualisation, using a manually-annotated overview of cell functions, assigned 1521 and 1227 DEGs to specific avocado processes and pathways in the SY vs AS and SY vs SG comparisons, respectively (Tables S7 and S8). The largest proportion of mapped DEGs (39% in both analyses) had roles in genetic information processing, including transcription (~20%), translation, protein modification (~8%), protein degradation (~8%), and RNA silencing. Genes involved in gene expression pathways were generally upregulated, with 63 – 76% of DEGs functioning in transcription, protein modification and protein degradation being induced in bleached tissues (Tables S7 and S8).

MapMan analysis also revealed a significant increase in expression of genes associated with plant immunity (represented as orange cell components in Fig. 2C and Fig. S1C). Over 34% of DEGs in SY tissues (with MapMan-assigned functions) had roles in pathways associated with biotic stress responses: calcium signalling, regulation of reactive oxygen species (ROS), expression of pathogenesis-related (*PR*) and nucleotide-binding site leucine-rich repeat (*NBS-LRR*) genes (shown together as "*R* genes" in Fig. 2C and Fig. S1C), as well as production of heat shock proteins (HSPs) and receptor-like kinases (RLKs). More than 85% of defence-related DEGs were upregulated in yellow tissues in both comparisons (Tables S7 and S8). Additionally, substantial upregulation of DEGs involved in phytohormone signalling, secondary metabolism, cell wall-related processes and transmembrane transport was observed, while photosynthesis was predominantly downregulated in bleached tissues (Fig. 2C, Fig. S1C).

To further investigate the relationship between suppression of photosynthesis and manifestation of bleaching symptoms, we examined the expression of nuclear-encoded chloroplastic genes in SY tissues using

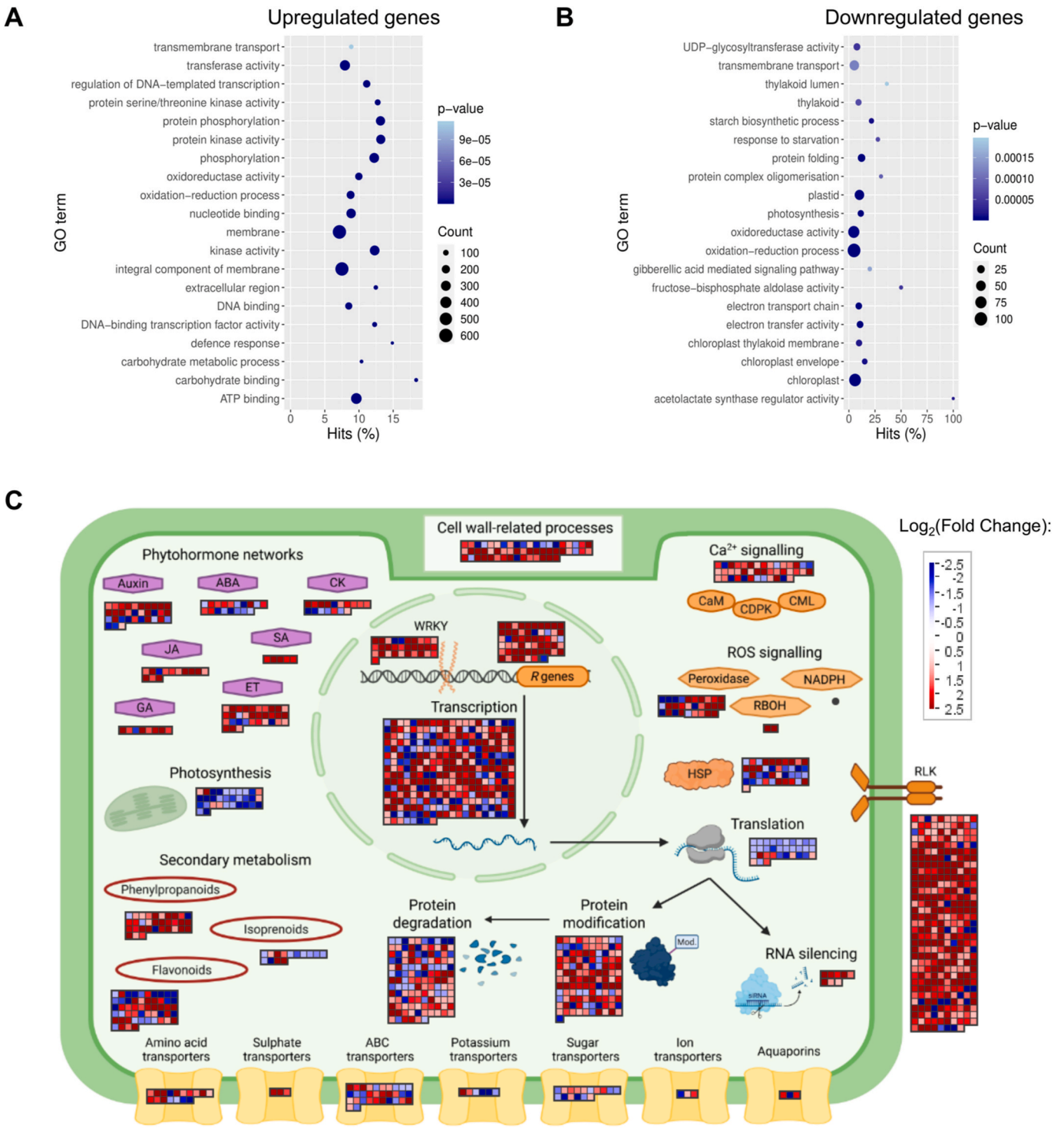

Fig. 2. Functional classification of genes differentially expressed (DEGs, *p*adj < 0.05; $|\log_2(\text{Fold Change})| \geq 1$) in yellow leaf sectors of bleached leaves (SY) compared to asymptomatic leaves (AS) in sunblotch-affected avocado trees. Top enriched gene ontology (GO) terms (over-represented *p*-value (FDR) < 0.05) are shown for DEGs which were significantly upregulated (**A**) or downregulated (**B**) in SY vs AS. Scatterplots show the proportion of DEGs, relative to the total annotated avocado genes in each category, on *x*-axes (Hits %), while the number of DEGs and FDR (*p*-value) are indicated by the corresponding legends. Further functional analysis used MapMan to assign DEGs to specific cellular pathways (**C**). DEGs belonging to specific pathways are indicated by individual coloured blocks, with transcript abundance shown as $\log_2$(Fold Change) in SY vs AS, coloured according to the scale provided (red = upregulated, blue = downregulated). Abbreviations: ABA—abscisic acid; ABC—ATP-binding cassette; CAM—calcium-binding calmodulin proteins; CDPK—calcium-dependent protein kinase; CK—cytokinin; CML—calmodulin-like protein; ET—ethylene; GA—gibberellic acid; HSP—heat shock protein; JA—jasmonic acid; *R* genes—nucleotide-binding site leucine-rich repeat (*NBS-LRR*) and pathogenesis-related (*PR*) genes; RBOH—respiratory burst oxidase homologue; RLK—receptor-like kinase; ROS—reactive oxygen species; SA—salicylic acid. (For interpretation of the references to colour in this figure legend, the reader is referred to the Web version of this article.)

additional MapMan analysis (Fig. 3, Fig. S2). Visualisation of DEGs assigned to photosynthesis- or chloroplast-specific functional bins by Mercator showed that 45 genes were downregulated in the SY vs AS comparison, whereas only seven of these genes were upregulated (Fig. 3). Downregulated photosynthetic genes visualised by MapMan were predicted to encode components of Photosystem II, Photosystem I, and the electron transport chain involved in the light reactions, as well as enzymes associated with the Calvin Cycle (Fig. 3, Fig. S2 and Table S9). Additionally, several DEGs encoding chloroplastic plastid ribosomal proteins (PRPs) and other chloroplast-targeted proteins showed reduced expression in bleached tissues, according to MapMan classification (Fig. 3, Fig. S2).

To identify photosynthesis-related DEGs that were not assigned to the corresponding functional bins by Mercator, we examined the Peame105 genome annotations for all DEGs identified in this study, with a focus on nuclear-encoded genes predicted to have chloroplastic functions. In addition to the 52 photosynthesis-associated DEGs visualised in MapMan, 90 chloroplast-targeted genes were differentially expressed in the SY vs AS comparison, of which 87% were downregulated (Table S9). Genes involved in photosynthesis were also downregulated when expression in yellow tissues (SY) was compared to expression in adjacent green sectors of the same leaves (SG), although to a lesser extent: a total of 74 chloroplast-related DEGs were significantly downregulated in SY vs SG (Table S9). These results correlated with findings of GO enrichment analysis, which showed strong bias toward photosynthesis-related functions among DEGs downregulated in yellow tissues relative to either of the green tissue types analysed in this study.

4. Discussion

In this study, we used RNA-seq to analyse global gene expression in a symptomatic avsunviroid-infected host for the first time. Transcriptome data were used to compare avocado gene expression in yellow sectors of bleached leaves (SY) with two sources of green leaf tissue from the same symptomatic ASBVd-infected trees: green sectors of bleached leaves (SG) and asymptomatic, fully green leaves (AS). Applying the criteria $p\text{adj} < 0.05$ and $\log_2\text{FC} \geq 1$ or ≤ -1, we identified 3169 DEGs in the SY vs AS comparison and 2512 DEGs in SY vs SG. These results demonstrate that leaf bleaching symptoms in ASBVd-infected avocado are associated with extensive reprogramming of host gene expression.

The scale of transcriptomic changes observed in bleached tissues is especially significant when compared to earlier observations of altered gene expression in asymptomatic ASBVd-infected trees. In our previous study, only 343 DEGs were identified using less stringent parameters ($p\text{adj} < 0.05$ and $|\log_2\text{FC}| \geq 0.58$), when comparing ASBVd-infected symptomless-carrier trees with uninfected trees (Joubert et al., 2024). In contrast, the present study revealed an almost tenfold increase in changes to gene expression when yellow tissues (SY) were compared to asymptomatic leaves (AS) from the same symptomatic trees. ASBVd was undetectable in most AS samples (two of three trees), consistent with prior reports of uneven systemic spread in sunblotch-affected trees, where viroid titres are markedly higher in symptomatic tissues than asymptomatic ones (Da Graca and Mason, 1983; Jooste and Zwane, 2021; Semancik and Szychowski, 1994; Vallejo-Pérez et al., 2014). Despite the higher ASBVd titre in SG samples relative to AS samples, only seven genes were differentially expressed in SG vs AS comparison. This shows that the extent of transcriptional reprogramming in ASBVd-infected avocado is more closely associated with host tissue phenotype than with the level of viroid accumulation in sampled leaves. Similar results have been observed in tomato infected with mild and severe variants of PSTVd, where symptom severity correlated with the number of DEGs, with severe infections inducing more changes to host gene expression than mild infections (Góra-Sochacka et al., 2019; Więsyk et al., 2018, 2020).

Comparison of DEGs in bleached tissues with those associated with asymptomatic infections of nursery trees (Joubert et al., 2024) revealed a number of genes with comparable expression profiles, where expression changes (up- or downregulation) for 61 DEGs in SY vs AS resembled those previously observed in the infected vs uninfected analysis (Joubert et al., 2024). Given the differences we observed in viroid titre in SY compared to AS samples in this study, it is likely that DEGs with similar expression in both symptomatic and asymptomatic infections are primarily affected by viroid load, and are unrelated to symptom expression. In contrast, 14 DEGs had conflicting expression profiles in SY vs AS compared to infected vs uninfected, representing candidates that are more likely associated with the development of bleaching symptoms. Future comparative global transcriptomic analyses of symptomatic avsunviroid-infected hosts and their uninfected counterparts will further clarify the relationship between viroid accumulation, disease severity, and host gene expression.

Functional classification of DEGs in SY samples revealed several cellular pathways with extensively modified gene expression in bleached leaf tissues. Genes involved in molecular expression pathways, particularly those associated with transcription, as well as protein

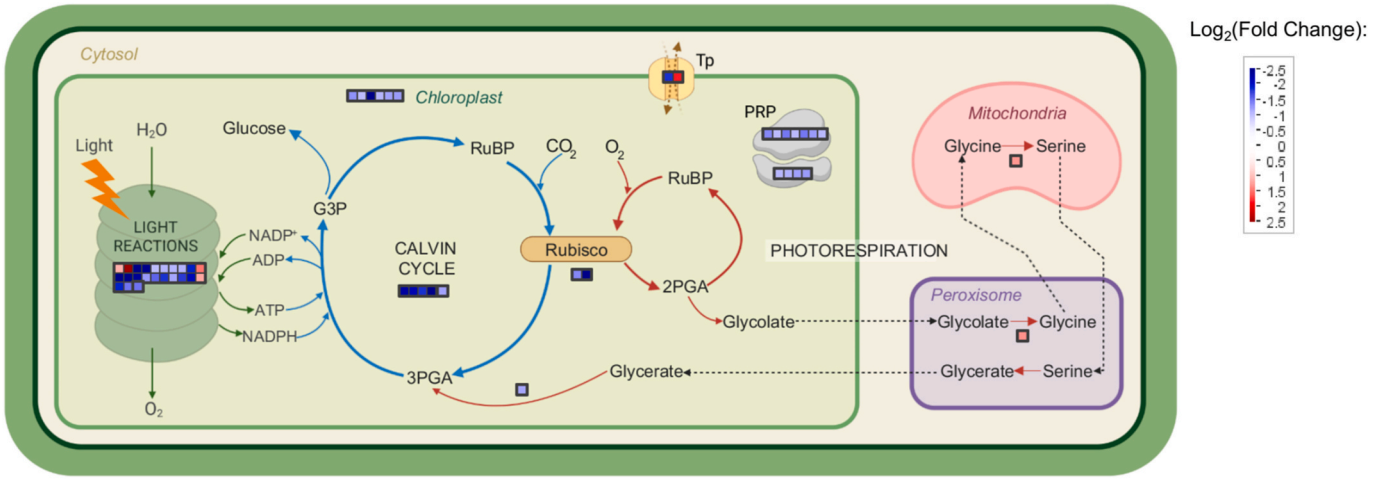

Fig. 3. MapMan visualisation of photosynthetic genes with differential expression (DEGs, $p\text{adj} < 0.05$; $|\log_2(\text{Fold Change})| \geq 1$) in yellow leaf sectors of bleached leaves (SY) relative to asymptomatic leaves (AS) in symptomatic ASBVd-infected trees. DEGs assigned to photosynthesis- or chloroplast-specific functional bins are visible as red (upregulated) or blue (downregulated) coloured blocks, with expression values displayed according to the accompanying scale. Abbreviations: G3P—Glyceraldehyde-3-phosphate; PGA—Phosphoglycerate; PRP—Plastid ribosomal protein (chloroplastic); RuBP—Ribulose bisphosphate; Tp—Transporter (chloroplastic). (For interpretation of the references to colour in this figure legend, the reader is referred to the Web version of this article.)

modification and kinase activity, were consistently and significantly upregulated in bleached tissues across all functional annotation approaches used in this study. MapMan analysis indicated that approximately 20% of all annotated DEGs in SY tissues were associated with transcription, the majority of which were upregulated. Altered expression of transcription factor (*TF*) genes has been reported in several other viroid-infected hosts (Hadjieva et al., 2021; Štajner et al., 2019; Wang et al., 2019; Więsyk et al., 2020; Xu et al., 2020), as well as in asymptomatic ASBVd-infected avocado (Joubert et al., 2024). Given the crucial role of TFs in modulating host gene expression (Spitz and Furlong, 2012), it is likely that modifications in *TF* expression contribute to the large-scale changes to the transcriptional landscape observed in bleached ASBVd-infected leaf tissues (Jakše et al., 2024).

The activity of TFs may be further influenced by their phosphorylation status, which is regulated by protein kinases (Weidemüller et al., 2021). We observed pronounced upregulation of genes encoding various protein kinases, with receptor-like kinases (*RLK*s) accounting for 19.8% of mapped DEGs in SY tissues. This altered accumulation of protein kinases likely contributes to global transcriptional changes by impacting cellular signalling networks in bleached ASBVd-infected tissues. Transcriptional cascades initiated by MAPKs and RLKs may, for example, influence expression of genes involved in phytohormone signalling networks and plant immunity (Clouse et al., 2011; Jagodzik et al., 2018; Zhu et al., 2023). Consistent with this, when excluding *RLK*s, more than 10% of DEGs in SY tissues were assigned to host defence-related functions by MapMan visualisation. Upregulation of plant immune response genes has been reported across all viroid-infected hosts for which global transcriptome data are available (Joubert et al., 2022). However, it remains unclear whether activation of host immunity is linked to cytopathic symptoms associated with viroid disease development (Jakše et al., 2024), or is merely a downstream effect of the initial molecular alterations triggered by viroid infection.

Functional classification of downregulated DEGs in bleached tissues revealed significant repression of nuclear-encoded genes functioning in photosynthesis, as well as genes encoding chloroplastic proteins, in SY samples. Disruption of photosynthesis was most noticeable when gene expression in yellow tissues was compared with asymptomatic leaves: GO enrichment, MapMan visualisation and annotation-based searches revealed more than 100 downregulated DEGs associated with photosynthesis- and chloroplast function in SY vs AS. These DEGs encoded components of the thylakoid membrane, Photosystems I and II, and chloroplastic ATP synthases, as well as proteins functioning in electron transport and carbon fixation. Consistent with these findings, reduced expression of photosynthesis-related genes has been reported in PSTVd-infected tomato (Więsyk et al., 2018, 2020) and pepper (Hadjieva et al., 2021), CEVd-infected 'Etrog' citron (Rizza et al., 2012), and CBCVd-infected hop (Mishra et al., 2018; Štajner et al., 2019), and was correlated with leaf chlorosis in these host-viroid interactions.

Early investigations of symptomatic ASBVd-infected avocado revealed that cells from the yellow regions of bleached leaves exhibited distinct changes in chloroplast structure and organisation, whereas chloroplasts in the green tissues of bleached leaves closely resembled those of healthy avocado leaves (Da Graca, 1979; Da Graca and Martin, 1981; Desjardins, 1987). The extensive downregulation of nuclear-encoded chloroplastic transcripts observed in SY samples relative to both SG and AS samples may underlie the malformation of chloroplasts previously observed in SY tissues, as reduced accumulation of chloroplastic proteins would be expected to directly compromise organelle structure. Furthermore, the suppression of multiple nuclear genes encoding subunits of chloroplastic PRPs may have cascading effects on chloroplast functions, as disrupted chloroplastic ribosome assembly could impact the translation of chloroplast genome-encoded transcripts. Consistent with this, reduced expression of nuclear genes encoding chloroplastic PRP subunits has been shown to induce yellowing or albinism phenotypes in transgenic arabidopsis, rice, and maize (Robles and Quesada, 2022). While our analysis was restricted to nuclear-encoded gene expression, future research should investigate the expression of chloroplast-encoded genes and the accumulation of chloroplastic proteins to clarify the link between disrupted chloroplast function and the development of leaf bleaching symptoms in avocado sunblotch disease.

Our data reveal a clear association between the downregulation of photosynthesis-related genes and disease development in ASBVd-infected leaves; however, the relationship between other large-scale transcriptomic changes and leaf bleaching is less distinct. The extensive gene expression changes observed in SY tissues is likely a downstream consequence of early ASBVd pathogenesis, potentially mediated through RNA silencing (Adkar-Purushothama et al., 2024; Flores et al., 2020; Joubert et al., 2025; Markarian et al., 2004). We previously demonstrated that SY tissues accumulate nearly 100 times more ASBVd-sRNAs than SG tissues, consistent with elevated viroid titres in symptomatic leaf sectors (Joubert et al., 2025). While targeting of avocado transcripts was not predicted for all the ASBVd-sRNAs detected in yellow tissues, it is likely that a number of these sRNAs hijack host RNA-silencing machinery to interfere with the expression of other avocado genes. This effect may be further amplified through the action of *trans*-acting siRNAs (Adkar-Purushothama et al., 2024; Adkar-Purushothama and Perreault, 2019; Gómez et al., 2009), potentially triggering additional signalling cascades in host cells, culminating in widespread transcriptional modifications in bleached ASBVd-infected tissues. Future studies should adopt integrated multi-omics approaches, such as those applied to HSVd-infected cucumber (Márquez-Molins et al., 2023), to compare the sRNAnome, methylome, transcriptome and degradome in symptomatic ASBVd-infection with uninfected avocado. Integrating these data with the gene expression analyses presented here will shed light on the interplay between RNA silencing, epigenetic regulation, and host gene expression underlying the development of avocado sunblotch disease.

5. Conclusions

This study represents the first global transcriptomic analysis of a symptomatic avsunviroid-infected host. Gene expression analysis revealed extensive reprogramming of the avocado transcriptome in yellow sectors of bleached ASBVd-infected leaves, compared to both the adjacent green sectors and the asymptomatic leaves from the same sunblotch-affected trees. The number of DEGs detected in bleached tissues was approximately ten times higher than that previously reported in asymptomatic ASBVd infection, indicating a strong correlation between the extent of transcriptional reprogramming and the phenotypic severity of ASBVd-infected leaf tissues. Functional classification highlighted widespread gene expression changes across multiple cellular pathways in bleached tissues, with pronounced alterations to molecular expression pathways, biotic stress responses, and photosynthesis. Notably, the coordinated downregulation of nuclear genes encoding chloroplastic proteins was strongly associated with bleaching symptoms, suggesting a potential link. Future investigations should extend similar transcriptomic analyses to symptomatic tissues of PLMVd-infected peach and CChMVd-infected chrysanthemum. Together with the findings presented here, such comparative studies will offer new insights into the host response to symptomatic avsunviroid infection and provide a more comprehensive understanding of the molecular interactions governing viroid-plant interactions.

Funding

This study was funded by the Hans Merensky Legacy Foundation.

CRediT authorship contribution statement

M. Joubert: Conceptualization, Data curation, Formal analysis, Investigation, Methodology, Visualization, Writing – original draft. **N.**

van den Berg: Conceptualization, Funding acquisition, Methodology, Supervision, Writing – review & editing. **J. Theron:** Supervision, Writing – review & editing. **V. Swart:** Conceptualization, Funding acquisition, Methodology, Supervision, Writing – review & editing.

Declaration of competing interest

The authors declare that they have no known competing financial interests or personal relationships that could have appeared to influence the work reported in this paper.

Acknowledgements

We are grateful to Alicia Clarke for creative input and Robert Backer for bioinformatic support. We also thank Macrogen Seoul for sequencing services.

Appendix A. Supplementary data

Supplementary data to this article can be found online at https://doi.org/10.1016/j.virol.2026.110903.

Data availability

Raw RNA-seq data are available from the Sequence Read Archive of NCBI Genbank under BioProject PRJNA1422735.

References

Adkar-Purushothama, C.R., Perreault, J.-P., Sano, T., 2024. Viroid-induced RNA silencing and its secondary effect on the host transcriptome. In: Adkar-Purushothama, C.R., Sano, T., Perreault, J.-P., Sreenivasa, M.Y., Di Serio, F., Daros, J.-A. (Eds.), Fundamentals of Viroid Biology. Academic Press, Cambridge, MA, USA, pp. 275–295.

Adkar-Purushothama, C.R., Perreault, J.P., 2019. Current overview on viroid–host interactions. Wiley Interdiscip. Rev. RNA 11, e1570.

Allen, R., Palukaitis, P., Symons, R., 1981. Purified avocado sunblotch viroid causes disease in avocado seedlings. Australas. Plant Pathol. 10, 31–32.

Backer, R., Engelbrecht, J., Van den Berg, N., 2022. Differing responses to *Phytophthora cinnamomi* infection in susceptible and partially resistant *Persea americana* (Mill.) rootstocks: a case for the role of receptor-like kinases and apoplastic proteases. Front. Plant Sci. 13, 928176.

Chi, S., Zhang, J., Li, H., Wang, P., Feng, L., Ren, Y., 2022. RNA-seq profiling reveals the transcriptional response against potato spindle tuber viroid in different potato cultivars and developmental stages. Potato Res. 1–12.

Clouse, S.D., Goshe, M.B., Huber, S.C., 2011. Phosphorylation and RLK signaling. In: Tax, F., Kemmerling, B. (Eds.), Receptor-Like Kinases in Plants: from Development to Defense. Springer, Berlin, Germany, pp. 227–251.

Da Graca, J., 1979. Avocado sunblotch. South African Avocado Growers' Association Research Report 3, 65–66.

Da Graca, J., Martin, M., 1981. Ultrastructural changes in avocado leaf tissue infected with avocado sunblotch. Phytopathol. Z. 102, 185–194.

Da Graca, J., Mason, T., 1983. Field indexing for avocado sunblotch disease. S Afr Avocado Growers' Assoc Yearbook 6, 83–85.

Delgado, S., Navarro, B., Serra, P., Gentit, P., Cambra, M.-Á., Chiumenti, M., De Stradis, A., Di Serio, F., Flores, R., 2019. How sequence variants of a plastid-replicating viroid with one single nucleotide change initiate disease in its natural host. RNA Biol. 16, 906–917.

Desjardins, P.R., 1987. Avocado sunblotch. In: Diener, T. (Ed.), The Viroids. Springer, pp. 299–313.

Di Serio, F., Li, S.-F., Matoušek, J., Owens, R.A., Pallás, V., Randles, J.W., Sano, T., Verhoeven, J.T.J., Vidalakis, G., Flores, R., 2018. ICTV virus taxonomy profile: *avsunviroidae*. J. Gen. Virol. 99, 611–612.

Di Serio, F., Owens, R.A., Li, S.-F., Matoušek, J., Pallás, V., Randles, J.W., Sano, T., Verhoeven, J.T.J., Vidalakis, G., Flores, R., 2021. ICTV virus taxonomy profile: *pospiviroidae*. J. Gen. Virol. 102, 001543.

Flores, R., Navarro, B., Delgado, S., Serra, P., Di Serio, F., 2020. Viroid pathogenesis: a critical appraisal of the role of RNA silencing in triggering the initial molecular lesion. FEMS Microbiol. Rev. 44, 386–398.

Gómez, G., Martínez, G., Pallás, V., 2009. Interplay between viroid-induced pathogenesis and RNA silencing pathways. Trends Plant Sci. 14, 264–269.

Góra-Sochacka, A., Więsyk, A., Fogtman, A., Lirski, M., Zagórski-Ostoja, W., 2019. Root transcriptomic analysis reveals global changes induced by systemic infection of *Solanum lycopersicum* with mild and severe variants of potato spindle tuber viroid. Viruses 11, 992.

Hadjieva, N., Apostolova, E., Baev, V., Yahubyan, G., Gozmanova, M., 2021. Transcriptome analysis reveals dynamic cultivar-dependent patterns of gene expression in potato spindle tuber viroid-infected pepper. Plants 10, 2687.

Jagodzik, P., Tajdel-Zielinska, M., Ciesla, A., Marczak, M., Ludwikow, A., 2018. Mitogen-activated protein kinase cascades in plant hormone signaling. Front. Plant Sci. 9, 1387.

Jakše, J., Wang, Y., Matoušek, J., 2024. Transcriptomic analyses provide insights into plant-viroid interactions. In: Adkar-Purushothama, C.R., Sano, T., Perreault, J.-P., Sreenivasa, M.Y., Di Serio, F., Daròs, J.-A. (Eds.), Fundamentals of Viroid Biology. Academic Press, Cambridge, MA, USA, pp. 255–274.

Jooste, A., Zwane, Z., 2021. Avocado sunblotch viroid (ASBVd) symptom identification and detection in avocado orchards. S Afr Avocado Growers' Assoc Yearbook 44, 66–71.

Joubert, M., van den Berg, N., Theron, J., Swart, V., 2022. Transcriptomics advancement in the complex response of plants to viroid infection. Int. J. Mol. Sci. 23, 7677.

Joubert, M., van den Berg, N., Theron, J., Swart, V., 2024. Global transcriptomic analysis in avocado nursery trees reveals differential gene expression during asymptomatic infection by avocado sunblotch viroid (ASBVd). Virus Res. 339, 199263.

Joubert, M., van den Berg, N., Theron, J., Swart, V., 2025. Small RNAs derived from avocado sunblotch viroid and their association with bleaching symptoms: implications for pathogenesis in avocado sunblotch disease. Arch. Virol. 170, 205.

Kuhn, D.N., Geering, A.D., Dixon, J., 2017. Avocado sunblotch viroid. In: Hadidi, A., Flores, R., Randles, J.W., Palukaitis, P. (Eds.), Viroids and Satellites. Academic Press, pp. 297–305.

Lohse, M., Nagel, A., Herter, T., May, P., Schroda, M., Zrenner, R., Tohge, T., Fernie, A.R., Stitt, M., Usadel, B., 2014. Mercator: a fast and simple web server for genome scale functional annotation of plant sequence data. Plant Cell Environ. 5, 1250–1258.

Markarian, N., Li, H., Ding, S., Semancik, J., 2004. RNA silencing as related to viroid induced symptom expression. Arch. Virol. 149, 397–406.

Mishra, A.K., Kumar, A., Mishra, D., Nath, V.S., Jakše, J., Kocábek, T., Killi, U.K., Morina, F., Matoušek, J., 2018. Genome-wide transcriptomic analysis reveals insights into the response to *citrus bark cracking viroid* (CBCVd) in hop (*Humulus lupulus* L.). Viruses 10, 570.

Márquez-Molins, J., Villalba-Bermell, P., Corell-Sierra, J., Pallás, V., Gomez, G., 2023. Integrative time-scale and multi-*omics* analysis of host responses to viroid infection. Plant Cell Environ. 46, 2909–2927.

Navarro, B., Gisel, A., Rodio, M.E., Delgado, S., Flores, R., Di Serio, F., 2012. Small RNAs containing the pathogenic determinant of a chloroplast-replicating viroid guide the degradation of a host mRNA as predicted by RNA silencing. Plant J. 70, 991–1003.

Palukaitis, P., Hatta, T., Alexander, D.M., Symons, R.H., 1979. Characterization of a viroid associated with avocado sunblotch disease. Virology 99, 145–151.

Posit Team, 2024. Rstudio: Integrated Development Environment for R. Posit Software. PBC, Boston, MA.

Rizza, S., Conesa, A., Juárez, J., Catara, A., Navarro, L., Duran-Vila, N., Ancillo, G., 2012. Microarray analysis of etrog citron (*Citrus medica* L.) reveals changes in chloroplast, cell wall, peroxidase and symporter activities in response to viroid infection. Mol. Plant Pathol. 13, 852–864.

Robles, P., Quesada, V., 2022. Unveiling the functions of plastid ribosomal proteins in plant development and abiotic stress tolerance. Plant Physiol. Biochem. 189, 35–45.

Schwacke, R., Ponce-Soto, G.Y., Krause, K., Bolger, A.M., Arsova, B., Hallab, A., Gruden, K., Stitt, M., Bolger, M.E., Usadel, B., 2019. MapMan4: a refined protein classification and annotation framework applicable to multi-omics data analysis. Mol. Plant 12, 879–892.

Semancik, J., Szychowski, J., 1994. Avocado sunblotch disease: a persistent viroid infection in which variants are associated with differential symptoms. J. Gen. Virol. 75, 1543–1549.

Serra, P., Navarro, B., Forment, J., Gisel, A., Gago-Zachert, S., Di Serio, F., Flores, R., 2023. Expression of symptoms elicited by a hammerhead viroid through RNA silencing is related to population bottlenecks in the infected host. New Phytol. 239, 240–254.

Spitz, F., Furlong, E.E., 2012. Transcription factors: from enhancer binding to developmental control. Nat. Rev. Genet. 13, 613–626.

Štajner, N., Radišek, S., Mishra, A.K., Nath, V.S., Matoušek, J., Jakše, J., 2019. Evaluation of disease severity and global transcriptome response induced by *Citrus bark cracking viroid, Hop latent viroid*, and their co-infection in hop (*Humulus lupulus* L.). Int. J. Mol. Sci. 20, 3154.

Takino, H., Kitajima, S., Hirano, S., Oka, M., Matsuura, T., Ikeda, Y., Kojima, M., Takebayashi, Y., Sakakibara, H., Mino, M., 2019. Global transcriptome analyses reveal that infection with chrysanthemum stunt viroid (CSVd) affects gene expression profile of chrysanthemum plants, but the genes involved in plant hormone metabolism and signaling may not be silencing target of CSVd-siRNAs. Plant Gene 18, 100181.

Vallejo-Pérez, M., Téliz-Ortiz, D., De La Torre-Almaraz, R., Valdovinos-Ponce, G., Colinas-León, M., Nieto-Ángel, D., Ochoa-Martínez, D., 2014. Histopathology of avocado fruit infected by Avocado sunblotch viroid. J. Agric. Sci. 6, 158.

Wang, Y., Wu, J., Qiu, Y., Atta, S., Zhou, C., Cao, M., 2019. Global transcriptomic analysis reveals insights into the response of 'Etrog' citron (*Citrus medica* L.) to *Citrus exocortis viroid* infection. Viruses 11, 453.

Weidemüller, P., Kholmatov, M., Petsalaki, E., Zaugg, J.B., 2021. Transcription factors: bridge between cell signaling and gene regulation. Proteomics 21, 2000034.

Więsyk, A., Iwanicka-Nowicka, R., Fogtman, A., Zagórski-Ostoja, W., Góra-Sochacka, A., 2018. Time-course microarray analysis reveals differences between transcriptional changes in tomato leaves triggered by mild and severe variants of potato spindle tuber viroid. Viruses 10, 257.

Więsyk, A., Lirski, M., Fogtman, A., Zagórski-Ostoja, W., Góra-Sochacka, A., 2020. Differences in gene expression profiles at the early stage of *Solanum lycopersicum*

infection with mild and severe variants of potato spindle tuber viroid. Virus Res. 286, 198090.
Xia, C., Li, S., Hou, W., Fan, Z., Xiao, H., Lu, M., Sano, T., Zhang, Z., 2017. Global transcriptomic changes induced by infection of cucumber *(Cucumis sativus* L.) with mild and severe variants of *hop stunt viroid*. Front. Microbiol. 8, 2427.
Xu, L., Zong, X., Wang, J., Wei, H., Chen, X., Liu, Q., 2020. Transcriptomic analysis reveals insights into the response to *hop stunt viroid* (HSVd) in sweet cherry (*Prunus avium* L.) fruits. PeerJ 8, e10005.
Young, M.D., Wakefield, M.J., Smyth, G.K., Oshlack, A., 2010. Gene ontology analysis for RNA-seq: accounting for selection bias. Genome Biol. 11, 1–12.
Zhu, Q., Feng, Y., Xue, J., Chen, P., Zhang, A., Yu, Y., 2023. Advances in receptor-like protein kinases in balancing plant growth and stress responses. Plants 12, 427.